# Role of Surface Tension in Fusion Welding (Part 3)†

## –Hydrodynamic Effect–

Akira MATSUNAWA*

**Abstract**

*The paper describes the liquid motions induced by the effect of surface tension. The first category of motion described is the liquid movements perpendicular to the surface that is originated by capillary pressure such as the rate of capillary rise and surface wave. The second one is the liquid motion parallel to the surface that is associated with the surface tension gradient on surface, which is sometimes called Marangoni effect, thermocapillary motion, or surface tension driven flow. In this article, some fundamental concepts of above motions are reviewed by employing simplified models.*

**KEY WORDS:** (Capillary Rise) (Surface Wave) (Marangoni Effect) (Convection) (Weld Pool) (Velocity Distribution) (Temperature Distribution)

## 1. Introduction

In the Part 1 and 2 of this series papers[1,2] were described the hydrostatic effect of surface tension on fusion welding phenomena such as bead surface profile, self sustaining of weld pool and droplet, and so on. However, the surface tension also plays very important roles in dynamic phenomena. In connection to fusion welding, there are several liquid motions induced by surface tension. They are basically classified into two characteristic motions. The first one is a motion perpendicular to the surface of liquid and the another is that parallel to the surface. The well known examples of the motion perpendicular to the surface are capillary rise and surface wave of liquid, which are caused by the capillary pressure originated by curved liquid surface.[3] The liquid motion parallel to the surface is not so well known but is also important phenomena particularly in relation to the spreading of active agents on liquid surface,[4] Bénard convection cells,[5–7,27] fireflame propagation of spread oil film on the sea,[8–11] and liquid circulation in welding molten pool.[12–22] The motive force of this kind of motion is the shearing stress associated by the difference of surface tension on free surface. Since the surface tension generally changes with temperature or amount of impurities, the gradient of surface tension is exerted on free surface if there exists temperature or constitutional distribution, and thus a surface tension driven flow is theoretically possible. In fact, the flow induced by surface tension is experimentaly verified in many organic compounds,[14–16] but, in actual welding pool of metals, no definite proof has been made yet if the surface tension driven flow is a main factor or not. In this paper, a systematic review will be carried on the liquid motion induced by surface tension.

## 2. Motions Perpendicular to Surface

### 2.1 Rate of capillary rise

Capillary rise is the most familiar motion of liquid induced by the effect of surface tension. In welding, too, the phenomenon plays an important role. Good examples are the penetration of flux and molten metal of soldering/brazing alloys into the very narrow gap or clearance.

In order to obtain the rate of capillary rise, let us suppose the following assumptions[3];

1) Let $a$ be the radius of cylindrical capillary,
2) the curvature of liquid interface is kept constant during motion and equal to $1/a$, and
3) the flow in the capillary is Hagen-Poiseuill flow,[23]

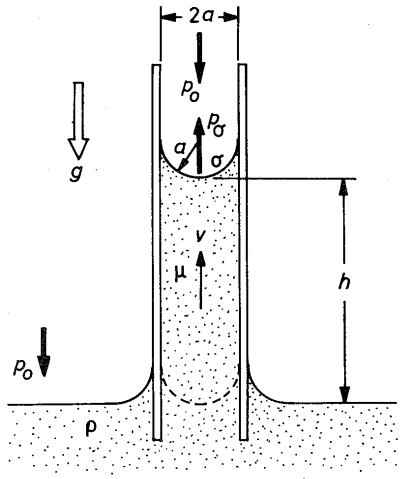


**Fig. 1** Pressure balance during capillary rise

† Received on April 30, 1984
* Associate Professor

Transactions of JWRI is published by Welding Research Institute of Osaka University, Osaka 567, Japan

i.e., a laminar flow at steady state. (See Appendix 1.)

As shown in **Figure 1**, the pressure balance equation is expressed as

$$\Delta p = p_\sigma - \rho g h \quad (1),$$

where, $p_0$ is the capillary pressure that was described in Part 1 and is written as

$$p_\sigma = \sigma \left( \frac{1}{R_1} + \frac{1}{R_2} \right) = \frac{2\sigma}{a} \quad (2).$$

The average speed of moving interface is

$$v = \frac{dh}{dt} = \frac{a^2}{8\mu} \frac{\Delta p}{h} \quad (3),$$

where, $\mu$ is the viscosity of liquid. (See Appendix 1.) Combining the equations (1) to (3), one leads to the following differential equation of motion.

$$\frac{dh}{dt} = \frac{a^2}{8\mu h} \left( \frac{2\sigma}{a} - \rho g h \right) \quad (4)$$

Integrating the above equation, one obtains

$$t = \frac{8\mu}{\rho g a^2} \left( h_0 ln \frac{h_0}{h_0 - h} - h \right) \quad (5),$$

where, $h_0$ is the final elevation of liquid and is given as

$$h_0 = \frac{1}{a} \frac{2\sigma}{\rho g} \quad (6).$$

However, the relation does not fit well in actual cases for small value of $t$, because the capillary rise is generally not a strict Hagen-Poiseulle flow. The equation (5) is, therefore, only valid for large value of $t$, i.e., when $t \gg \rho a^2/\mu$. If the more accurate solution is required, one has to consider a transient phenomenon at the biggining of motion. A simplified explanation of transient flow in tube is given in the Appendix 2.

The above is the case that a capillary is placed perpendicularly. If a capillary is placed horizontally, the gravity term in the equation (4) can be neglected. Denoting $l$ be the horizontal distance, the equation becomes

$$\frac{dl}{dt} = \frac{\sigma a}{4\mu l} \quad (7),$$

and thus

$$t = \frac{2\mu l^2}{\sigma a} \quad (8),$$

or

$$l = \sqrt{\frac{\sigma a t}{2\mu}} \quad (9).$$

Namely, the penetration depth of liquid into capillary is proportional to $\sqrt{\sigma a t/\mu}$.

### 2.2 Surface wave

Surface wave in molten pool has been interested in relation to the surface rippling of bead or some potential-ful information for automatic control of fusion welding.[24] However, their mechanisms in real molten puddle are very complicated and no systematic research is found in the literature.

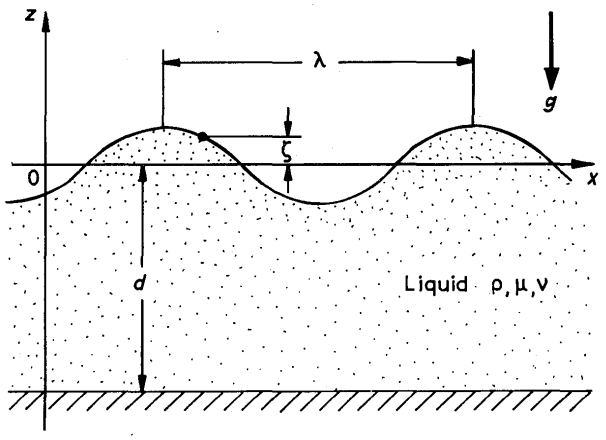


**Fig. 2** Wave on free surface of liquid

In fluidmechanics, there are two distinct waves depending on the ratio between the wavelength and liquid depth as described in **Figure 2.** Namely, the wave having much smaller wavelength than the depth of liquid is called "Surface Wave" and another case is "Tidal Wave". In this section, only a basic concept of surface wave will be reviewed, though the actual wave in weld puddle, particularly in the vicinity of pool edge, contain both surface and tidal waves. Detailed theories of waves are seen in literatures.[3,25]

Basic equations that governs the wave phenomena are; Navier-Stokes equation:

$$\frac{\partial \mathbf{v}}{\partial t} + (\mathbf{v}\, grad)\, \mathbf{v} = -\frac{1}{\rho} grad\, p + \nu \Delta \mathbf{v} + \mathbf{g} \quad (10)$$

Continuity equation:

$$div\, \mathbf{v} = 0 \quad (11)$$

A non-linear equation (10) can be linearized under the following appropriate assumptions;

(1) Viscosity term $\nu\Delta\mathbf{v}$ in equation (10) is small enough compared with acceleration term $\partial\mathbf{v}/\partial t$.
(2) The term $(\mathbf{v}grad)\,\mathbf{v}$ is small compared to $\partial\mathbf{v}/\partial t$.
(3) The wave propagates $x$-direction only (Two dimensional wave).

The assumption (1) is equivalent to that

$$\frac{\omega\lambda^2}{\nu} \gg 1 \quad (12),$$

where, $\lambda$: wavelength,
$\omega$: wave frequency, and
$\nu$: kinematic viscosity ($= \mu/\rho$).

Similarly, the assumption (2) is equivalent to that the wave amplitude $a$ is very small compared to wavelength, i.e.,

$$a \ll \lambda \quad (13),$$

or equivalent to small Reynolds number, i.e.,

$$\frac{a}{\lambda}\frac{\omega\lambda^2}{\nu} \ll 1 \quad (14).$$

Therefore, the equation (10) is simplified to

$$\frac{\partial \mathbf{v}}{\partial t} = -\frac{1}{\rho} grad\, p + \mathbf{g} \quad (15),$$

$x$-component:

$$\frac{\partial v_x}{\partial t} = -\frac{1}{\rho}\frac{\partial p}{\partial x} \quad (15a),$$

$z$-component:

$$\frac{\partial v_z}{\partial t} = -\frac{1}{\rho}\frac{\partial p}{\partial z} - g \quad (15b).$$

The boundary conditions under the consideration are;

a) Wave motion is confined to a shallow region (Assumption 2), thus

$$\mathbf{v} \to 0 \quad \text{as} \quad z \to -\infty \quad (16).$$

b) The pressure on the free surface of liquid (wave surface) must be equal to the gas pressure above liquid, thus

$$p + p_\sigma = p_0 \quad \text{at} \quad z = \varsigma(x, t) \quad (17),$$

where, $p_0$ : gas pressure above liquid,
$p_\sigma$ : capillary pressure

$$\left(p_\sigma = \frac{\sigma}{R} = \sigma\frac{\partial^2 \varsigma}{\partial x^2}\right), \text{ and}$$

$\varsigma(x, t)$ : wave profile.

Under the above boundary conditions, one can obtain the solutions of equations (11), (15a) and (15b) as follows;
Wave frequency:

$$\omega^2 = \frac{8\pi^3\sigma}{\rho\lambda^3} + \frac{2\pi g}{\lambda} \quad (18)$$

Phase velocity of the wave:

$$C = \frac{\lambda\omega}{2\pi} = \sqrt{\frac{2\pi\sigma}{\rho\lambda} + \frac{\lambda g}{2\pi}} \quad (19)$$

Velocity components:

$$v_x = a\omega e^{\kappa z} sin\,(\kappa x - \omega t) \quad (20)$$
$$v_z = -a\omega e^{\kappa z} cos\,(\kappa x - \omega t) \quad (21)$$

where, $\kappa = \frac{2\pi}{\lambda}$ : wave number.

Pressure:

$$p = -\rho g z + \frac{\rho a\omega^2 e^{\kappa x}}{\kappa} sin\,(\kappa x - \omega t) \quad (22)$$

Wave profile on the liquid surface:

$$\varsigma = a\, sin\,(\kappa x - \omega t) \quad (23)$$

$a$ : wave amplitude

It is noted in equation (18) that the wave frequency consists of independent terms of surface tension and gravity. If the gravity term is much greater than the capillary term, i.e.,

$$\lambda \gg 2\pi\sqrt{\sigma/(\rho g)} \quad (24),$$

the wave is called "Gravity Wave" and its wave parameters are expressed as

$$\omega = \sqrt{2\pi g/\lambda} = \sqrt{g\kappa} \quad (25),$$

and

$$C = \sqrt{\lambda g/(2\pi)} = \sqrt{g/\kappa} \quad (26).$$

On the contrary, when the capillary term is much greater than the gravity term, the surface oscillation is called "Capillary Wave" and its parameters become as follows.

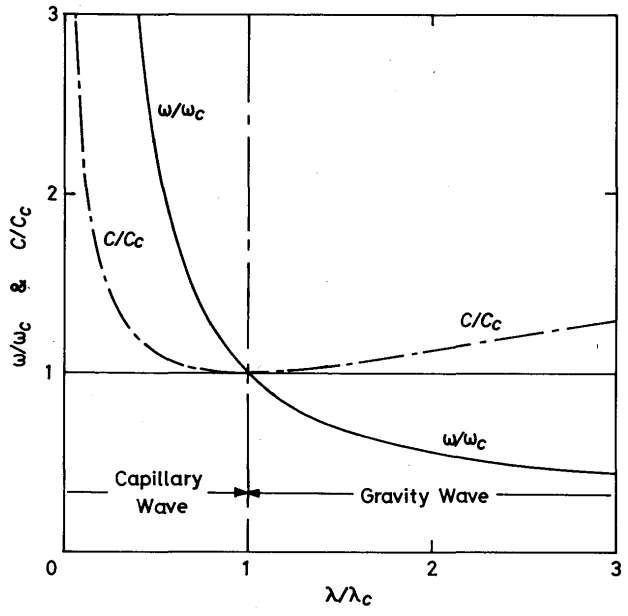


Fig. 3 Propagation characteristics of gravity and capillary waves

$$\omega = \sqrt{8\pi^3\sigma/(\rho\lambda^3)} = \sqrt{\sigma\kappa^3/\rho} \quad (27)$$

$$C = \sqrt{2\pi\sigma(\rho\lambda)} = \sqrt{\sigma\kappa/\rho} \quad (28)$$

In **Figure 3** are shown the propagation characteristics of gravity and capillary waves. The wave frequency decreases with the increase in wavelength, while the phase velocity of wave has the minimum value at the characteristic wavelength of

$$\lambda c = 2\pi\sqrt{\sigma/(\rho g)} = \sqrt{2}\,\pi h^* \approx 4h^* \quad (29),$$

where, $h^* = \sqrt{2\sigma/(\rho g)}$ (Capillary constant).

This characteristic wavelength is featured by the capillary constant. Namely, if the wavelength is much less than the four times of capillary constant of the liquid, the wave is regarded as capillary wave, and another case is gravity wave. As stated in the Part 1 of this series paper, molten metals usually have very high capillary constants and thus the effect of gravity wave is not significant for weld puddles having the size around 10 mm or so.

Refering to equations (18) and (19), it is interesting to note that accurate measurement of surface tension is possible if one measures the wavelength, wave frequency and phase velocity simultaneously.

## 3. Motion Parallel to Surface

### 3.1. General view of Marangoni effect

In previous sections have been discussed the liquid motions in case of uniform surface tention distribution. Here, let us discuss a case that the surface tension varies place to place on the liquid surface. As the surface tension is a kind of contraction force, the surface having higher surface tension attracts that having lower surface tension, and liquid motion takes place parallel to the surface.

As mensioned in the Sections 1 and 4 of previous Part 1 report[1], the surface tension of one component system is the function of temperature and surface area, and its temperature coefficient is always negative. Therefore, if there exists temperature gradient over the liquid surface, there appears surface tension gradient, which means that tangential force or shearing force is exerted along the surface and a surface flow takes place. If the liquid is confined in a small basin, the induced surface flow causes a convection in the entire basin due to the viscosity of liquid.

This kind of surface tension driven flow was first predicted theoretically by Marangoni[26] in 1871 and hence it has been called Marangoni effect or thermocapillary motion. However, the phenomenon had been long ignored because the natural convection was regarded more dominant. For instance, a cellular convective motion that observed in the case of fluid layers heated from below, which was often called Bénard cells, was usually ascribed to the instability of the density gradient, i.e., unstable natural convection, but, in 1958, Pearson[27] concluded that surface tension was more responsible than buoyancy force for many Bénard cell type motions. Levich[3] dealt a precise theoretical analysis of thermocapillary motion in his book in 1962, and criterion of motion due to surface tension and gravity force was clarified. In 1972, an experiment on the mechanism of Bénard cells was conducted in gravity free space by NASA using Apollos 14 and 17, and it was concluded that the cellular convective motion was due to the surface tension effect.[5–7]

In the field of welding, Ishizaki and his colleagues[12–15] proposed in 1965 that the formation of peripheral penetration that observed in a low current stationary TIG arc welding was due to the liquid circulation induced by surface tension. They also conducted a demonstration experiment using the paraffin as a bath and soldering iron as a heater and observed that high speed radial flow which took place on the free surface from the center to periphery developed to the entire circulation of paraffin pool which resulted in the similar penetration shape obtained in a TIG arc experiment as shown in **Figure 4**. This concept brought a hot discussions, but there still left

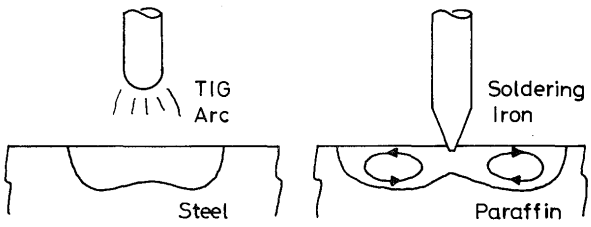


**Fig. 4** Penetration shape of stationary TIG arc weld and demonstration experiment of liquid circulation in paraffin pool melted by soldering iron

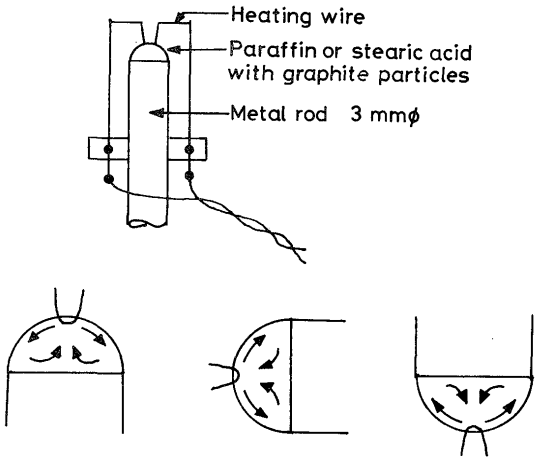


**Fig. 5** Effect of droplet direction to gravitaional field on liquid circulation

some doubt that the natural convection might be more influential. In 1971, Anderson[16] conducted a subtle experiment as shown in **Figure 5** to proove the existence of surface tension streaming and its influence by gravity on earth. He found that circulation in a small droplet of organic compound did not change by the direction of droplet to gravity. Bless[17] carried out a theoretical analysis of surface tension driven flow in shallow pool and showed that the calculated surface flow speed could be considerably high in liquid iron. Both Anderson and Bless supported the existence of surface tension driven flow in organic compounds, but they concluded that thermocapillary motion was unprobable in actual weld pool because the surface contamination by oxygen or other impurities included in metals would decrease the surface tension drastically which might result in actually no gradient of surface tension in spite of the existence of temperature distribution.

Recently, Heiple and others[18,19] observed that if a small amount of surface tension decreasing elements such as Selenium, Sulpher and others were locally added in the base metal, an opposite direction flow took place in weld puddle at the place where minor elements were located. This interesting phenomenon was interpreted by them that the local concentration of these minor elements at higher temperature region was less than that at lower temperature site due to de-adsorption effect which caused higher surface tension at the center part of weld pool. By this fact, the surface tension driven flow has been again spotlighted worldwide. In 1983, Yokoya and Matsunawa[20,21] conducted numerical analyses of surface tension induced flow in semicylindrical and hemispherical basins and clarified the stream and temperature fields, and similar work was published by Oreper and others[22] in 1983.

### 3.2. Velocity and temperature fields in surface tension driven flow

In order to obtain a clear view of surface tension driven flow, let us first consider a two dimensional rectangular basin filled with liquid as shown in **Figure 6.**[17] As the surface tension changes with temperature, tangential force along the surface appears if there exists temperature gradient.

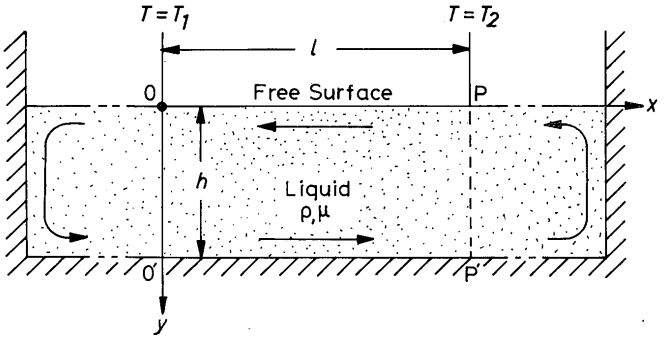


Fig. 6 Shallow basin model of surface tension driven flow

$$p_t = grad\ \sigma = \frac{\partial \sigma}{\partial T}\ grad\ T \tag{30}$$

$$(\frac{\partial \sigma}{\partial T} < 0 \text{ for single component system})$$

If one supposes that the points 0 and P in **Fig. 7** are kept constant temperatures $T_1$ and $T_2$ respectively and the temperature gradient along the surface is linear, then

$$\sigma = \sigma(T_1) + (\frac{\partial \sigma}{\partial T})\ \frac{T_2 - T_1}{\ell}\ x \tag{31}$$

Let us also suppose that the liquid depth is small and there is no temperature gradient along $y$-direction. Then, the velocity component of $y$-direction can be ignored in the region between 0-0′ and P-P′. Navier-Stokes equation at steady state is expressed as

$$\frac{\partial p}{\partial x} = \mu(\frac{\partial^2 v_x}{\partial x^2} + \frac{\partial^2 v_x}{\partial y^2}) \tag{32}.$$

The assumption of small depth leads to

$$\frac{\partial v_x}{\partial x} \ll \frac{\partial v_x}{\partial y}.$$

Therefore, equation (32) is simplified as

$$\frac{\partial p}{\partial x} = \mu \frac{\partial^2 v_x}{\partial y^2} \tag{33}.$$

Furthermore, the pressure may not be considered as the function of $y$ because of small $h$.

$$\frac{\partial p}{\partial y} \approx 0$$

Hence, the continuity equation is expressed as

$$\int_0^h v_x dy = 0 \tag{34},$$

and the boundary conditions are

$$(v_x)_{y=h} = 0 \tag{35},$$

$$\mu(\frac{\partial v_x}{\partial y})_{y=0} = p_t = \frac{\partial \sigma}{\partial T}\ grad\ T \tag{36}.$$

Integrating equation (33) and also considering that the pressure (tangential force) changes only in $x$-direction, one obtains

$$v_x = a + by + \frac{1}{2\mu}\frac{dp}{dx}y^2.$$

Substituting the boundary conditions, $v_x$ is given as

$$v_x = \frac{1}{\mu}\frac{\partial \sigma}{\partial x}(h-y) - \frac{1}{2\mu}\frac{dp}{dx}(h^2-y^2) \quad (37).$$

Putting equation (37) into equation (35),

$$\frac{dp}{dx} = \frac{3}{2h}\frac{\partial \sigma}{\partial x} \quad (38),$$

and final solution of $v_x$ is thus obtained as

$$v_x = \frac{1}{4\mu h}\frac{\partial \sigma}{\partial T}(3y-h)(y-h)\frac{dT}{dx} \quad (39),$$

Velocity at surface:

$$(v_x)_{y=0} = \frac{1}{4\mu}\frac{\partial \sigma}{\partial T} h \frac{dT}{dx} \quad (40),$$

Maximum velocity of reverse flow;

$$(v_x)_{y=2h/3} = -\frac{1}{12\mu}\frac{\partial \sigma}{\partial T} h \frac{dT}{dx} \quad (41).$$

**Figure 7** shows the calculated velocity profile. The velocity is proportinal to both liquid depth and temperature gradient. However, the above calculation was based on the assumption of small value of $h$, which is equivalent to that the momentum change in $x$-direction is much less than that of the viscous force in $y$-direction, i.e.,

$$v_x \frac{\partial v_x}{\partial x} \ll \nu \frac{\partial^2 v_x}{\partial y^2}$$

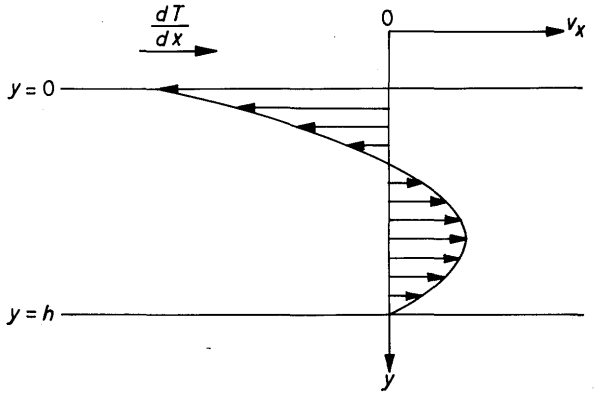


**Fig. 7** Calculated velocity profile of surface tension driven flow in shallow basin

As the liquid depth and length are $h$ and $\ell$ respectively,

$$\frac{v_x^2}{\ell} \ll \frac{\nu |v_x|}{h^2}$$

i.e.,

$$h^2 \ll \frac{\nu \ell}{|v_x|} \quad (42),$$

or combining equations (42) with (40),

$$h^3 \ll \frac{4\nu^2 \rho \ell}{\left|\frac{\partial \sigma}{\partial T}\right|\left|\frac{dT}{dx}\right|} \quad (43).$$

Namely, the equations (39), (40) and (41) are only valid when all the parameters satisfy the relation (43).

The above was an analytical model of surface tension driven flow in shallow basin. However, the linear modelling was too much simplified to apply to actual weld pool. The more detailed calculations have been conducted numerically by the author[20,21], and Oreper and others[23]. The flow and temperature fields in semicylindrical and hemispherical basins were obtained by solving principal equations of fluid-mechanics, i.e., Navier-Stokes, continuity and energy equations using the idea of stream function. The calculations are rather complex, and here only important results will be briefed in case of two dimensional case.

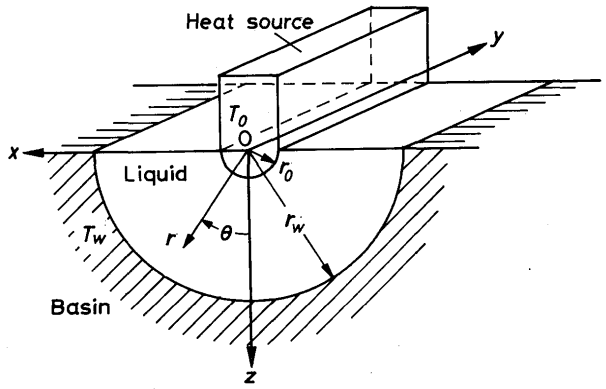


**Fig. 8** Convection model of surface tension driven flow in semicylindrical basin

**Figure 8** shows a convection model, where the liquid is contained in a semicylindrical basin whose wall temperature is kept constant and a semicylindrical heat source or sink of constant but different temperature is immersed in the liquid at the center. Similar to Bless' calculation,[17] the flow is assumed laminar in the whole basin and also the temperature coefficient of surface tension is taken to be constant. Here, let introduce the following nondimensional parameter:

$$\Lambda = \frac{\lambda r_w (T_0 - T_w)}{\rho \nu^2} \quad (44),$$

where, $\lambda$ : Temperature coefficient of surface tension ($\lambda = -\partial\sigma/\partial T$),
$r_w$ : Radius of basin,
$T_w$: Wall temperature of basin,
$T_0$ : Temperature of heat source/sink,
$\rho$ : Density of liquid, and
$\nu$ : Kinetic viscosity.

Supposing a pure iron bath, the dimensionless temperature coefficient of surface tension $\Lambda$ is related to the actual basin size and temperature difference as tabulated in **Table 1**.

**Figure 9** shows some typical calculated patterns of flow and temperature fields for various values of $\Lambda$. The flow velocity increases with the increase in $\Lambda$, and the convection grows stronger in the entire region of basin. Due to this fluid motion, the temperature contours are

**Table 1** Basin sizes and temperature differences and corresponding $\Lambda$-values

| $r_w$ | $\Delta T = T_0 - T_w$ | $\Lambda$ |
|---|---|---|
| 0.005 m | 2℃ | $2\times10^3$ |
| 0.005 m | 20℃ | $2\times10^4$ |
| 0.005 m | 50℃ | $5\times10^4$ |
| 0.005 m | 100℃ | $10^5$ |
| 0.005 m | 200℃ | $2\times10^5$ |

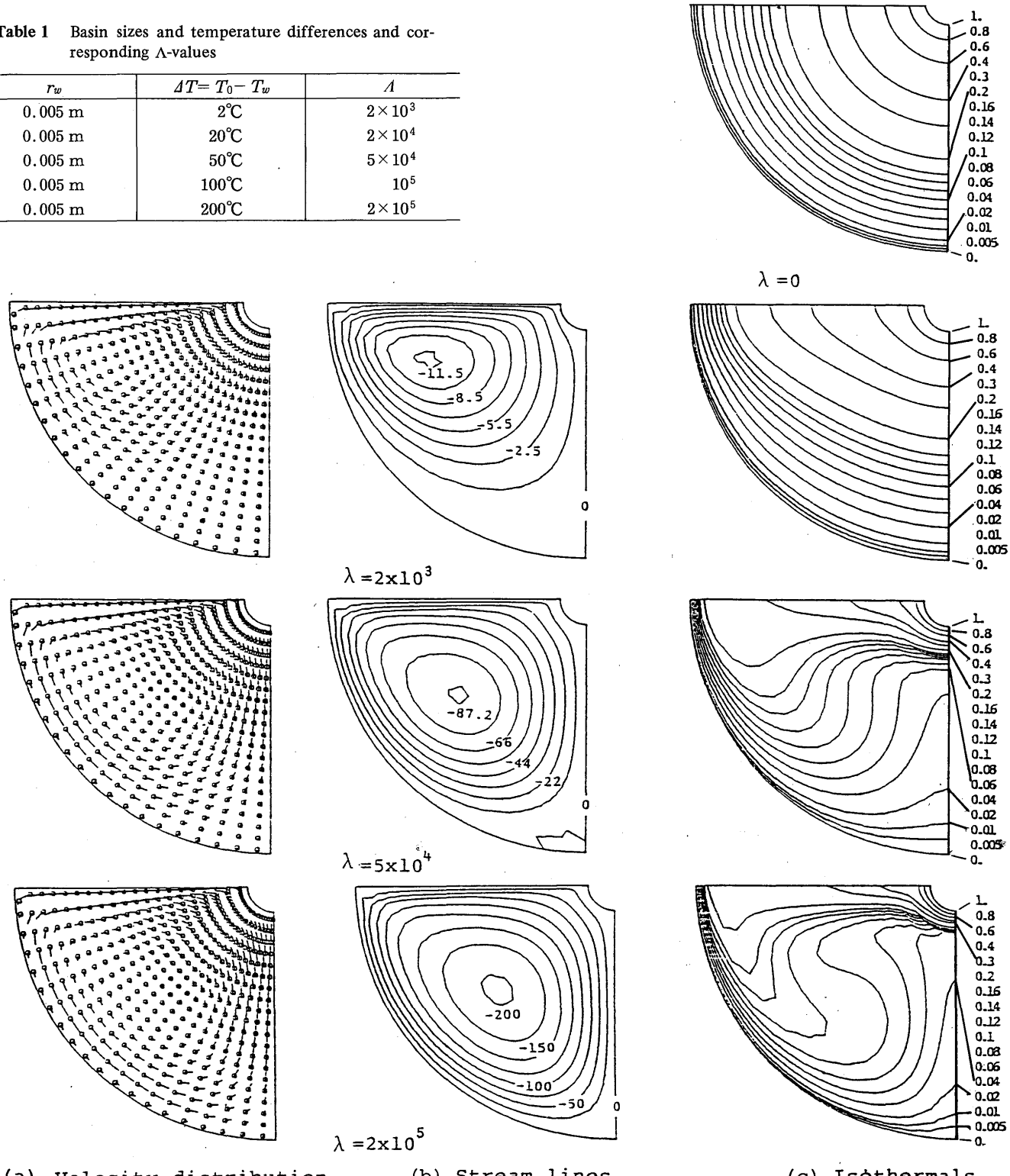


**Fig. 9** Calculated flow and temperature fields for various values of $\Lambda$

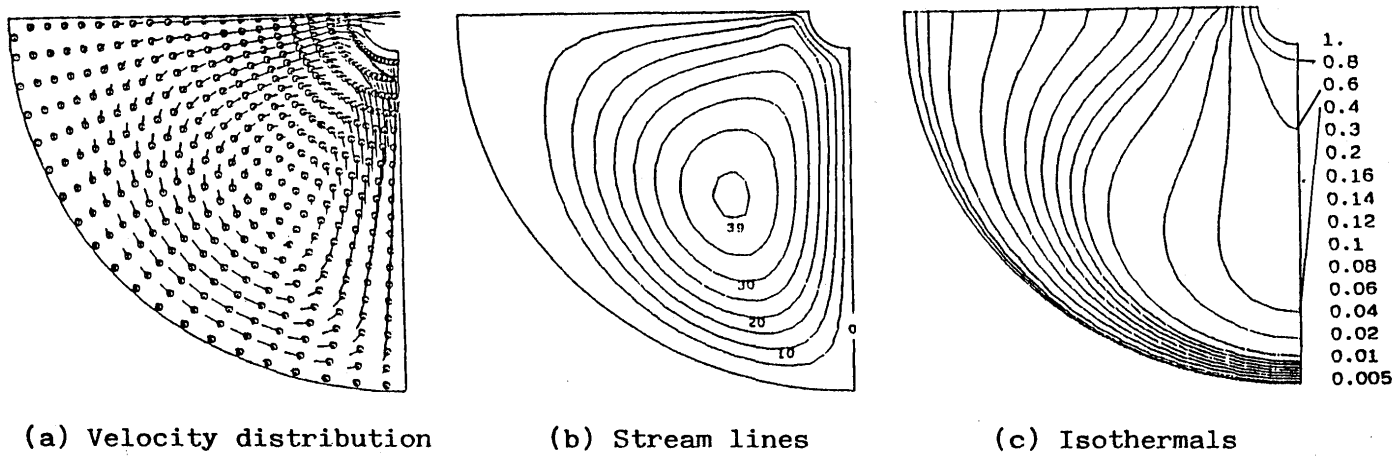


**Fig. 10** Flow and temperature fields in case of positive temperature coefficient of surface tension

deformed considerably from those of heat conduction type at low value of $\Lambda$ to very distorted profiles at higher value of $\Lambda$. Particularly, the low temperature profile resembles to a penetration shape of Ishizaki's paraffin pool.[14] (Figure 5)

As described above, the outward radial streaming takes place on the liquid surface if the high temperature source stays at the center and the temperature coefficient of surface tension is negative, i.e., positive $\Lambda$. If the reverse motion that Heiple and others[18,19] reported were due to the migration effect of impurities depending on temperature, namely higher surface tension at higher temperature, the phenomenon may be analogous to that when the surface tension has a positive temperature coefficient, i.e., negative $\Lambda$ value in the above model. **Figure 10** is an example of such situation, in which one sees that the downward speed of flow along the center line is considerably high and the equitemperature contours are pear or pendant drop shapes, which suggest a deep penetration is achievable in reverse motion of flow.

In **Figures 11** and **12** are presented the velocity and temperature distributions on the free surface in both cases of negative and positive temperature coefficient of surface tension. When the stream is directed to periphery, the

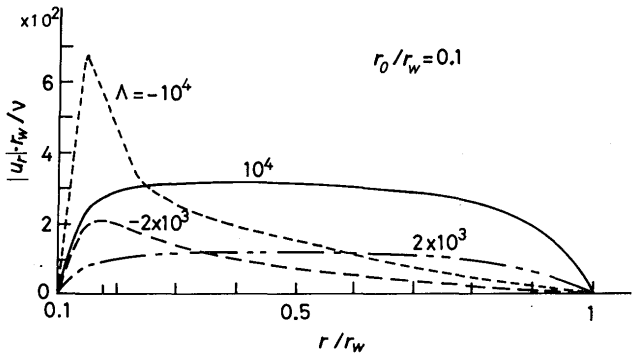


**Fig. 11** Velocity distribution on free surface and its dependence on flow direction

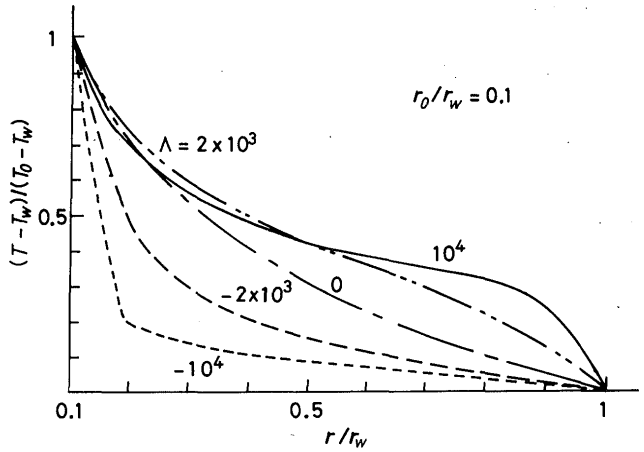


**Fig. 12** Temperature distribution on free surface and its dependence on flow direction

flow is accelerated at the heat source region and decelerated at the periphery and the flow speed is kept almost constant in the middle part of surface. While, when the flow is converged to the center, the stream is gradually accelerated from the periphery to center and remarkably accelerated and steeply decelerated in the vicinity of heat source. These velosity fields well reflect to the thermal field as seen in Figure 12. It should be noted here that the temperature distribution is rather flat in wide area of surface if streaming takes place and only steep distribution is observed near the heat source or basin wall depending on the direction of motion. This means that the driving force of motion by surface tension is mainly associated near the heat source or sink.

**Figure 13** shows the nondimensional heat flux intensity distribution along the basin wall. Due to the heat transfer by convection, the heat is more effectively transfered to the periphery of basin in case of outward flow, while the basin bottom is more heated in case of inward streaming. In the figure, the total heat input is different depending on the flow intensity, because the constant temperature

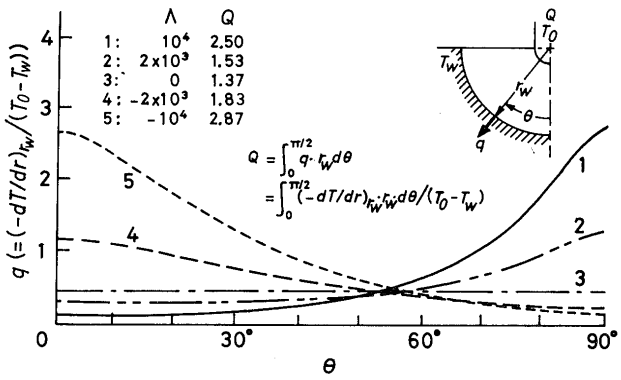


**Fig. 13** Heat flux distribution along basin wall

difference was assumed in the model. The nondimensional heat input $Q$ shown in Figure 14 is calculated by integrating the heat flux intensity along the basin wall.

## 4. Summary

Liquid motions induced by the effect of surface tension were reviewed in this paper, in which were described two types of movements depending on the direction of motion to the surface. The motive forces of motion are different in both cases, namely, the capillary pressure is the driving force in case of movement parpendicular to the surface, while the tangential or shearing force is main factor in case of motion parallel to the surface. As the purpose of this series papers were to emphasize the importance of surface tension in fusion welding, the used concepts and modelings were too much simplified and thus the indivisual result might not always explain the actual phenomena in welding but still the author wishes that this articles would be helpful to further clarification of complicated welding phenomena. For example, the actual motion in welding pool from the view point of surface tension theory itself is the combination of surface wave and convection to which one has to consider the both motions perpendicular and parallel to the surface. Of course, the weld pool phenomena are not only governed by surface tension but also influenced greatly by airodynamic forces, electromagnetic force and others. Now, we have already stepped into a new era to clarify the quantitative contribution of each factor to the phenomena, and there we must not forget the role of surface tension.

## Acknowledgement

The series articles were based on the lecture note of Graduate School of The Welding Engineering Department at Ohio State University, U.S.A., when the author was a Visiting Professor in 1980 and 1981. The author wishes to express his gratitude to Prof. K. Graff, Chairman of the Department, for his suggestion and encouragement of publishing these papers. He also appreciates to Prof. S. Yokoya of Nippon Institute of Technology for his collaboration in the field of computor simulation of surface tension driven flow.

## References

1) A. Matsunawa and T. Ohji; "Role of Surface Tension in Fusion Welding (Part 1)", Trans. JWRI, Vol. 11, No. 2 (1982) p. 145.

2) ibid.; "ibid (Part 2)", ibid., Vol. 12, No. 1 (1983) p. 123.

3) V.C. Levich; Physicochemical Hydrodynamics, Prentice-Hall, Englewood Cliffs (1962), Chapter VII, p. 372.

4) J.T. Davies and E.K. Rideal; Interfacial Phenomena, Academic Press, New York (1963), Chapter 1, p. 1.

5) P.G. Grodzka, et al.; "The Apollo 14 Heat Flow and Convection Demonstration Experiments", Report of Lockheed Missiles and Space Company, Huntsville Research and Engineering Center, HREC-5577-3, LMSC-HREC D 225333, Sep., 1971.

6) T.C. Bannister; "Heat Flow and Convection Demonstration (Apollo 14), NASA Technical Memorandum, NASA TM X-64735, March, 1973.

7) T.C. Banister, et al.; "Apollo 17 Heat Flow and Convection Experiments, Final Data Analyses Results", NASA Technical Memorandum, NASA TM X-64772, July, 1973.

8) H. Isoda; Study of Mechanics, 23-11, Nov. (1971), p. 1505, p. 1598 (in Japanese).

9) K.E. Torrance; Comb. Sci. Technol., 3-3, No. 5 (1971), p. 133.

10) Y. Matsumoto and T. Saito; Trans. Japan Soc. Mech. Eng., 46-402 (1980), p. 282.

11) N. Shinmen, et al.; 17th Japan Heat Transfer Symposium, May (1980), p. 127 (in Japanese).

12) K. Ishizaki, et al.; "Interfacial Tension Theory on the Phenomena of Arc Welding, No. 9", J. Japan Welding Society (JWS), Vol. 34, No. 2 (1965), p. 146 (in Japanese).

13) ibid.; "Mechanism of Penetration in Arc Welding", IIW SG 212 Doc. (1965).

14) ibid.; "Penetration Pehnomena of Organic Solid", J. JWS, Vol. 36, No. 4 (1967), p. 416 (in Japanese).

15) ibid.; "Penetration in Arc Welding and Convection in Molten Metal", IIW SG 212, Doc. 212-77-66 (1966).

16) D. Anderson; "Streaming due to a Thermal Surface Tension Gradient", IIW SG 212, Doc. 212-217-71 (1971); Doc. 212-177-73 (1973).

17) S.J. Bless; "Surface Tension Streaming", IIW SG 212, Doc. 212-235-72 (1972).

18) C.R. Heiple and J.R. Roper; "Effect of Selenium on GTAW Fusion Zone Geometry", W.J., Aug. (1981), p. 143-s.

19) ibid.; "Mechanism for Minor Element Effect on GTA Fusion Zone Geometry", W.J., April (1982), p. 97-s.

20) S. Yokoya, Y. Asako & A. Matsunawa; "Surface Tension Driven Flow in Semicylindrical Basin", Trans. J.W.S., Vol. 14, No. 2, October (1983), p. 135.; IIW SG 212, Doc. 212-563-83 (1983).

21) S. Yokoya and A. Matsunawa; "Surface Tension Driven Flow

in Hemispherical Basin", J. JWS (to be published in Japanese).

22) G.M. Oreper, T.W. Eager & J. Szekely; "Convection in Arc Weld Pools", W.J., November (1983), p. 307-s.

23) W.H. Giedt; Principles of Engineering Heat Transfer (Japanese Translation), Maruzen Publishing Co., 1960.

24) R.J. Renwick & R. Richardson; "Experimental Investigation of GTA Weld Pool Oscillation", W.J., Vol. 62, No. 2 (1983), p. 29-s.

25) H. Lamb; Hydrodynamics, Cambridge University Press

26) C. Marangoni; Ann. Phys. Chem., 143, p. 337 (1871). (Refer to J. Szekely; Fluid Flow Phenomena in Metals Processing, Academic Press, New York (1979).

27) J.R.A. Pearson; "On Convection Cells Induced by Surface Tension", J. Fluid Mech., Vol. 4 (1958), p. 489.

28) H.L. Langhaar; "Steady Flow in the Transition Length of a Straight Tube", J. Applied Mechanics, 64, June (1942), A 55-58.

## Appendixes

### 1. Hagen-Poiseulle Flow

A cylindrical laminar flow of viscous fluid at steady state is called Hagen-Poiseulle flow in which the pressure drop between sections 1 and 2 in **Figure A1** is balanced with the opposite shearing stress along the side surface of cylindrical element of liquid column. The velocity profile in pipe shows parabolic distribution and its average speed is the half of the maximum one.

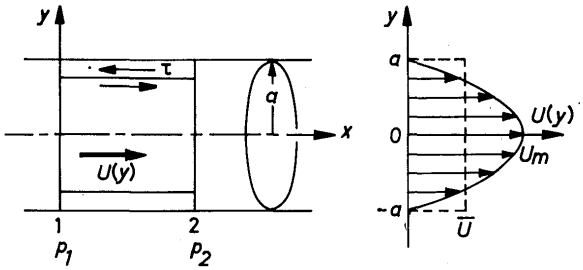


**Fig. A1** Hagen-Poiseulle flow

$$\Delta p = p_1 - p_2$$

$$\Delta p \cdot \pi y^2 + 2\pi y \ell \mu \frac{du}{dy} = 0$$

$$\therefore du = -\frac{\Delta p}{2\pi \ell} y dy$$

Integrating the above under the conditions of $u = 0$ at $y = a$,

$$u = \frac{\Delta p}{4\mu \ell}(a^2 - y^2)$$

Average speed $\overline{u}$ is then

$$\overline{u} = \frac{1}{\pi a^2} \int_0^a u \cdot \pi y dy = \frac{\Delta p}{8\mu \ell} a^2.$$

### 2. Transient Flow at Tube Entrance

When the fluid enters into a tube with uniform velocity distribution as shown in **Figure A2**, the radial velocity

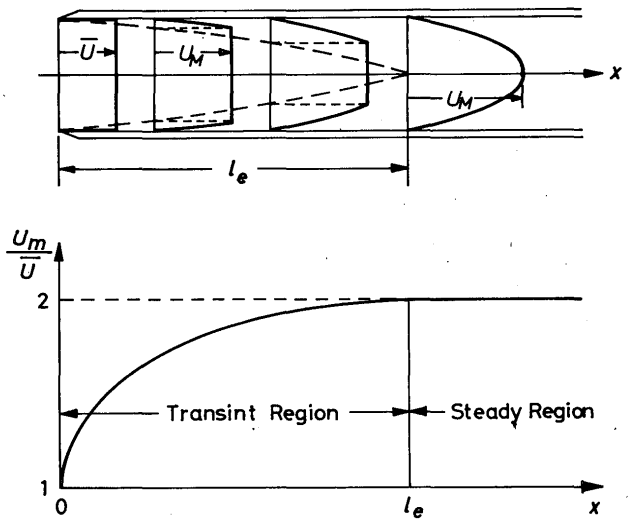


**Fig. A2** Transient flow at tube entrance (only schematic)

profile changes as the fluid proceeds due to the development of boundary layer along the tube wall from starting section, and the flow finally develops to Hagen-Poiseulle flow when the boundary layer thickness becomes the tube radius. This unsteady distance is called "Transient", "Accelerating" or "Starting" region in which the flow is accelerated and reaches twice of the initial speed at the end of the region.[28] The length of transient region is given as below.

$$\ell_e/a \approx 0.05 a\overline{u}/\nu = 0.05Re$$

or

$$\ell_e \approx 0.05 a^2 \overline{u}/\nu$$